Planta (2004) 220: 17–29
DOI 10.1007/s00425-004-1323-5

ORIGINAL ARTICLE

Sheng-Bing Wang · Feng Chen · Milton Sommerfeld
Qiang Hu

Proteomic analysis of molecular response to oxidative stress by the green alga *Haematococcus pluvialis* (Chlorophyceae)

Received: 25 March 2004 / Accepted: 28 May 2004 / Published online: 17 July 2004

Abstract Rapidly growing, green motile flagellates of *Haematococcus pluvialis* can transform into enlarged red resting cysts (aplanospores) under oxidative stress conditions. However, it is not known what initial molecular defense mechanisms occur in response to oxidative stress, and may ultimately lead to cellular transformation. In this study, global-expression profiling of cellular proteins in response to stress was analyzed by two-dimensional gel electrophoresis, image analysis, and peptide mass fingerprinting. Oxidative stress was induced in cultures of green flagellates by addition of acetate and Fe^{2+}, and exposure to excess light intensity. Overall, 70 proteins were identified with altered expression patterns following stress induction. Some key proteins involved in photosynthesis and nitrogen assimilation were down-regulated, whereas some mitochondrial respiratory proteins were transiently up-regulated after the onset of stress. Most of the identified proteins, particularly those from the families of superoxide dismutase, catalase, and peroxidase, were transiently up-regulated, but reverted to down-regulation during the 6 days of stress. On the other hand, cellular accumulation of the antioxidant astaxanthin occurred well after initiation of oxidative stress and reached its maximum cellular level after six or more days of stress. It appears that the early stress response involves multiple enzymatic defense processes that play a critical role upon onset of stress and also during the early transition of green vegetative cells to red cysts. As cyst development continues, the intensive, enzyme-mediated initial responses were largely replaced in mature red cysts by accumulation of the molecular antioxidant astaxanthin. This study provides the first direct evidence for a massive, and concerted up-regulation of multiple antioxidative defense mechanisms, both spatially and temporarily, to protect *H. pluvialis* cells against oxidative stress.

Keywords Astaxanthin · *Haematococcus* · Oxidative stress · Protein expression · Proteomics · Stress response

Abbreviations 2-DE: Two-dimensional gel electrophoresis · IPI: Isopentenyl-diphosphate δ-isomerase · HSP: Heat-shock protein · MALDI–TOF: Matrix-assisted laser desorption/ionization–time of flight · ROS: Reactive oxygen species · SOD: Superoxide dismutase

Introduction

Photosynthetic microalgae, like higher plants, generate reactive oxygen species (ROS) such as H_2O_2, O_2^- and $^{\bullet}OH$ through chloroplast photosynthesis and mitochondrial respiration (Asada 1994). ROS may play both destructive and constructive roles in cell growth and development. On the one hand, ROS may act as strong oxidants to damage various cellular components (Asada 1994). On the other hand, ROS may serve as efficient signaling molecules to trigger and mediate cell defense systems to improve resistance and adaptation of microalgae and plants to an unfavorable environment (Kobayashi et al. 1993; Desikin et al. 2001; Mittler 2002). During normal aerobic metabolism, the generation and detoxification of ROS in the cell remain in equilibrium. However, biotic and abiotic stimuli may unbalance the equilibrium, resulting in so-called "oxidative stress" (i.e., overproduction of ROS) that may lead to reduced growth and productivity, and even cell death under severe circumstances (Foyer and Mullineaux 1994).

To counter the deleterious processes caused by ROS, microalgae and plants have evolved a number of

S.-B. Wang · M. Sommerfeld · Q. Hu (✉)
School of Life Sciences, Arizona State University,
Tempe, AZ 85287-4501, USA
E-mail: huqiang@asu.edu
Tel.: +1-480-9656376
Fax: +1-480-9656899

S.-B. Wang · F. Chen
Department of Botany, the University of Hong Kong,
Pokfulam Road, Hong Kong, P.R. China

defensive mechanisms that both repair the various types of damage and scavenge toxic ROS. The major ROS-scavenging pathways include superoxide dismutase (SOD), ascorbate-specific peroxidase and catalase, and occur in various cellular compartments (Mittler 2002). In addition, a number of low-molecular-mass antioxidants, such as ascorbic acid, glutathione, carotenoids and tocopherols, can be actively involved in quenching ROS (Blokhina et al. 2003).

The unicellular green alga *Haematococcus pluvialis* can accumulate large amounts of the red keto-carotenoid astaxanthin under various environmental stress conditions, such as high light stress, salt stress, and deprivation of nutrients, either singly or in combination (Boussiba 2000; Steinbrenner and Linden 2001). A number of carotenoid biosynthesis genes, such as isopentenyl diphosphate isomerase (Sun et al. 1998), phytoene synthase (Steinbrenner and Linden 2001), phytoene desaturases (Grünewald et al. 2000), lycopene β-cyclase (Steinbrenner and Linden 2003), β-carotene ketolase (Lotan and Hirschberg 1995; Breitenbach et al. 1998), and carotenoid hydroxylase (Linden 1999), have been cloned and at least partially characterized in this organism. A common feature of these carotenoid genes is that their expression undergoes transient up-regulation with maximum mRNA transcript levels occurring 24–48 h after the onset of stress induction, followed by vigorous biosynthesis and cellular accumulation of astaxanthin, with a maximum level reached after 6–12 days of stress (Boussiba et al. 1999; Zhekisheva et al. 2002). It has been generally assumed that the accumulation of astaxanthin is a survival strategy of this organism and other related organisms in response to stressful environments (Boussiba 2000).

However, our understanding of the molecular defense mechanisms of *H. pluvialis* in response to oxidative stress is incomplete. This is particularly true for early events involved in antioxidative defense processes prior to the cellular accumulation of astaxanthin, and visible morphological and cellular structural changes. Although possible involvement of antioxidative enzymes in the stress response of *H. pluvialis* may be anticipated, no protein of this type has ever been isolated and characterized. One attempt was made by Kobayashi et al. (1997) who conducted an assay for SOD using *H. pluvialis* whole-cell and cell-free extract samples. A cDNA encoding a serine protease heat-shock protein (htrA) was isolated from *Haematococcus* under stress, but no attempt was made to isolate the htrA (Hershkovits et al. 1997). Recently, we developed an improved two-dimensional gel electrophoresis (2-DE) protocol (Wang et al. 2003), and introduced a proteomic approach to study cell wall proteins of *H. pluvialis* (Wang et al. 2004). We demonstrated that 2-DE coupled with peptide mass fingerprinting (PMF) is a viable approach for identification of homologous proteins across species boundaries, making it possible for positive identification of proteins from *H. pluvialis*, an organism whose genome has yet to be sequenced.

The aim of this study was to systematically survey the molecular response of *H. pluvialis* to oxidative stress, with a special emphasis on the early molecular defense events occurring prior to and/or during the transition from stress-sensitive green vegetative cells to stress-resistant red cysts. Global expression profiling of the cellular soluble proteome of *H. pluvialis* in response to stress was analyzed, using 2-DE and a matrix-assisted laser desorption/ionization–time of flight (MALDI–TOF) mass spectrometry-based PMF method. The results demonstrated that the early stress response involves multiple enzymatic defense processes that may play a critical role in protecting cells from oxidative damage before a long-term survival strategy involving cellular accumulation of astaxanthin and cyst formation is fully established.

Materials and methods

Organism, growth medium and culture conditions

Haematococcus pluvialis Flotow NINE144 was obtained from the National Institute for Environmental Studies in Tsukuba, Japan. An acetate basal medium described by Kobayashi et al. (1991) was used: 14.6 mM sodium acetate, 2.7 mM L-asparagine, 2 g l^{-1} yeast extract, 0.985 mM $MgCl_2$, 0.135 mM $CaCl_2$, 0.036 mM $FeSO_4$, pH 6.8. The cells were grown in 1,000-ml Erlenmeyer flasks each containing 500 ml growth medium. Cultures were incubated in a growth chamber (model: 1-35LLVL; Percival, Boone, IA, USA) at 22°C and 20 μmol photons m^{-2} s^{-1} of light under a 12 h light/12 h dark cycle. Cultures were shaken manually once each day. For stress induction, exponentially growing cultures (cell density of approximately 5×10^5 cells ml^{-1}) were spiked with 45 mM sodium acetate and 450 μM ferrous sulfate ($FeSO_4$). Cultures were then exposed to continuous illumination of 150 μmol photons m^{-2} s^{-1}.

Cell counting and pigment analysis

The cell number was determined using a hemacytometer under a light microscope. HPLC analysis of pigments was done according to the method of Yuan et al. (1997). Briefly, algal cells were harvested and extracted in the solvent mixture of dichloromethane and methanol (25:75, v/v). Pigment analysis was conducted on a liquid chromatograph equipped with two 510 pumps and a 996 photodiode array (PDA) detector (Waters, Milford, MA, USA). Pigment extracts (20-μl aliquots) were separated and analyzed using an Ultrasphere C_{18} column (250 mm long, 4.6 mm i.d.; 5 μm; Beckman Instruments, Fullerton, CA, USA) at 25°C. The mobile phase consisted of methanol (69.0%), dichloromethane (17.0%), acetonitrile (11.5%), and water (2.5%). The flow rate was 1.0 ml min^{-1}. A three-dimensional chromatogram was recorded from 300 to 700 nm. Peaks

were measured at a wavelength of 450 nm to facilitate the simultaneous detection of chlorophylls and carotenoids. Chromatographic peaks were identified by comparing retention times and spectra against known standards or by comparing their spectra with published data.

Preparation of *H. pluvialis* cellular soluble proteins

Culture suspension (500 ml) was taken at various time intervals and the cells were harvested by centrifugation (3,000 *g*, 5 min) and washed three times with cold deionized water. Cellular soluble proteins were prepared as describe in Wang et al. (2003).

Two-dimensional gel electrophoresis (2-DE) and image analysis

Details of 2-DE with *H. pluvialis* were described in a previous study by Wang et al. (2003). The basal solubilization buffer contained 2 M thiourea, 8 M urea, 4% CHAPS, 20 mM DTT, and 0.2% carrier ampholytes (Bio-lytes 3–10). Sample entry was made through in-gel rehydration. A total of 300 µl of solubilization buffer containing 250 µg protein sample was incubated with the IPG (immobilized pH gradient) gel strips (pH 3–10 linear gradients or pH 5–8 linear gradients, 17 cm; Bio-Rad) at 20°C for 15 h.

SDS–PAGE gels were stained with a Bio-safe Coomassie stain solution (Bio-Rad, Hercules, CA, USA). Gels were scanned with a Fluor-S multilmager system (Bio-Rad). The images were exported to TIFF format and imported to the PDQuest 2-D Analysis Software (Bio-Rad) and Z_3 software (Compugen, Tel Aviv, Israel).

In-gel digestion and peptide extraction

In-gel digestion was carried out using Montage in-gel digest$_{96}$ kits (Millipore, Bedford, MA, USA) with minor modifications as described in a previous study by Wang et al. (2004).

Matrix-assisted laser desorption/ionization–time of flight (MALDI–TOF) mass spectrometry (MS)

Peptides were solubilized in 10 µl of 0.1% trifluoroacetic acid (TFA) and loaded on previously equilibrated (in 50% acetonitrile followed by 0.1% TFA) ZipTip $_{\mu}$C18 pipette tips (Millipore). Tips were washed with 0.1% TFA and peptides were eluted with 2 µl saturated α-cyano-4-hydroxycinnamic acid in 50% acetonitrile/0.1% TFA directly on a metal MALDI–TOF target plate and allowed to dry. MALDI–TOF–MS spectra were acquired and recorded with a Voyager-DE STR mass spectrometer (PerSeptive Biosystems, Framingham, MA, USA) using an accelerating voltage of 20 kV in reflector mode and using a software macro for mass peak detection, noise reduction and de-isotoping. Internal mass calibration was performed using trypsin autodigestion products (842.51 Da and 2211.11 Da).

Protein identification by database searches

Peptide mass fingerprints generated by MALDI–TOF MS for each sample were matched to the theoretical tryptic digests of proteins from the NCBI database (National Center for Biotechnology Information, release 4 June 2003) using the MS-Fit software through the UCSF Mass Spectrometry Facility, San Francisco (http://prospector.ucsf.edu), and ProFound software through http://prowl.rockefeller.edu/cgi-bin/ProFound. Taxonomic category was first set to green plants; organisms across species boundaries were selected if no positive identification was made by this narrow species entry. Searches were carried out under guidance of the experimental molecular weight of individual proteins resolved on the 2-D gel. Mass accuracy was set at ± 50 ppm for most MALDI–TOF analyses with a minimum requirement of four peptides matched. The maximum number of missed cleavages was set at one. Possible post-translational modifications such as oxidation of methionine, *N*-terminal acetylation, *N*-terminal pyroglutamic acid, and modification of cysteine by acrylamide, were taken into consideration for queries. The database search output had a number of matched proteins ranked according to their MOWSE score, the mass error margin, and the sequence coverage by matched peptides.

Results

Morphological changes of *H. pluvialis* under stress

Using light microscopy we observed that 4-day-old cultures grown under favorable conditions were comprised predominantly of small green vegetative flagellates ranging in diameter from 8 µm to 16 µm (Fig. 1a). When 45 mM acetate and 450 µM Fe^{2+} were added to an exponentially growing culture and the culture transferred from light intensity of 20 to 150 µmol photons m^{-2} s^{-1}, the vegetative cells underwent noticeable pigment and morphological changes. Motile flagellates changed from green to yellow/brown color within 24 h and then to orange/red after three more days (Fig. 1b). The combination of high light and excessive amounts of acetate and Fe^{2+} stimulated the formation and reproduction of red motile flagellates for a period of 2–3 days. For example, over 70% of the cells were in the red, vigorously motile flagellated form in the 3-day-old culture. The vigorous reproduction of red motile flagellates under certain stress conditions has been reported pre-

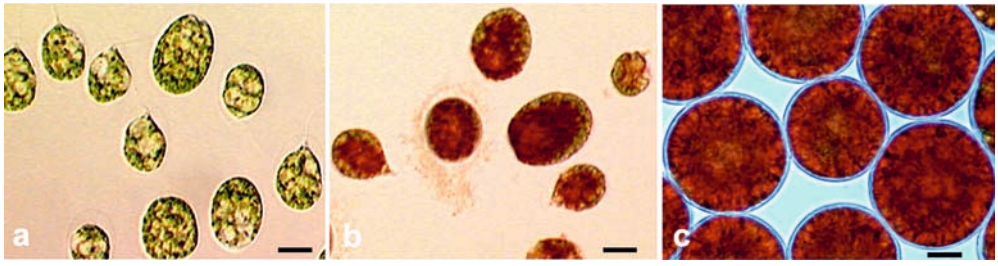

Fig. 1a–c Light micrographs of *Haematococcus pluvialis* at different stages of the cell cycle. **a** 4-day-old culture under favorable growth conditions (the cells were in fresh basal growth medium at 20°C and light of 20 μmol photons m^{-2} s^{-1}). **b** 3-day-old culture under stress conditions (i.e., 150 μmol photons m^{-2} s^{-1}, 45 mM sodium acetate and 450 μM Fe^{2+}). **c** 6-day-old culture under stress conditions. Bars = 10 μm

viously by other researchers (Grunewald et al. 1997), which is somewhat in conflict with the general belief that stress may result in immediate cessation of cell division in this organism (Boussiba 2000). However, as stress persisted, red flagellates gradually transformed into red cysts that became enlarged, developed a thickened cell wall with a noticeable intervening space between the cell wall and protoplast, and accumulated numerous lipid bodies in the cytoplasm (Fig. 1c). After 6 days of stress induction, almost all red flagellates became mature large red cysts 30–50 μm in diameter.

Cell growth and pigment profiling of *H. pluvialis* under stress

Figure 2a shows the changes in population density of *H. pluvialis* after onset of stress, starting from 4-day-old green vegetative cell cultures. Cell number increased gradually from 4.4×10^5 cells ml^{-1} to 6.1×10^5 cells ml^{-1} during the first 3 days of stress induction and leveled off afterwards. Some cell death was observed as stress persisted, as indicated by the occurrence of bleached cells and cell wall skeletons, which resulted in a slight decline in cell number after 3 days of stress. Cell death under similar stress conditions was also observed by Kobayashi et al. (1993), who reported a 20% decrease in cell number after 5 days of stress.

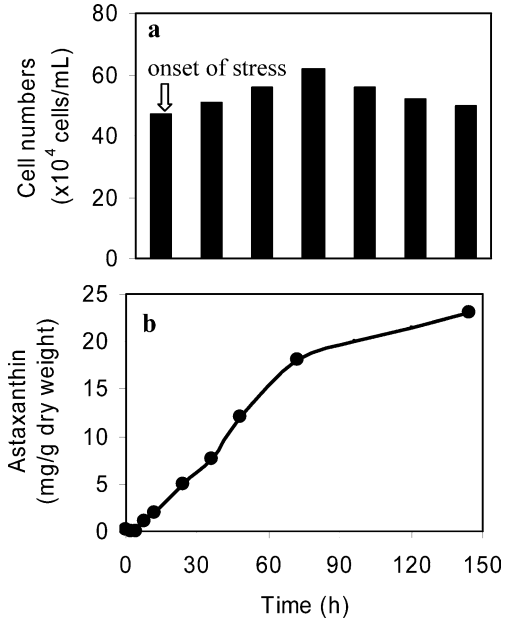

Fig. 2a, b Cell numbers (**a**) and cellular astaxanthin accumulation (**b**) of *H. pluvialis* during stress induction. Data represent mean values of three independent cultures

Figure 2b shows the cellular accumulation of astaxanthin during the transformation of green vegetative cells to red flagellates and cysts under stress. While little astaxanthin was present in the cells during the first 8 h of stress, astaxanthin began to accumulate in a linear mode between 12 h and 72 h and continued to increase slightly over the 6 days (144 h) of stress. This induction pattern agrees with that observed by Kobayashi et al. (1991, 1993). Recently, Steinbrenner and Linden (2001) showed that the induction of carotenoid hydroxylase, a key enzyme involved in astaxanthin biosynthesis, occurred at 8 h, corresponding to our earliest detection of astaxanthin formation.

Analysis of cellular proteome following oxidative stress

Soluble protein extracts from cultures at defined time intervals following stress induction were analyzed by 2-DE, and protein maps in triplicate produced from three independent protein extractions showed a high level of reproducibility. Figure 3 is a representative 2-D map of soluble proteins extracted from green vegetative cells, in which approximately 900 well-defined protein spots in the pI region of 3–10 were detected by Coomassie Blue staining. In an analytical gel, which was loaded with the same protein sample and stained with silver, ca. 1,500 spots were visualized in the same pI region (data not shown).

In order to classify cellular protein expression profiles, a systematic comparison of 2-D maps of soluble proteins extracted during the transformation of green vegetative cells to red cysts was made with Z_3 software (Compugen). Although spot matching was done automatically, distorted spots were corrected by manual addition of 'registration anchors' (Smilansky 2001). Table 1 summaries five specific expression patterns of cellular soluble proteins in response to oxidative stress.

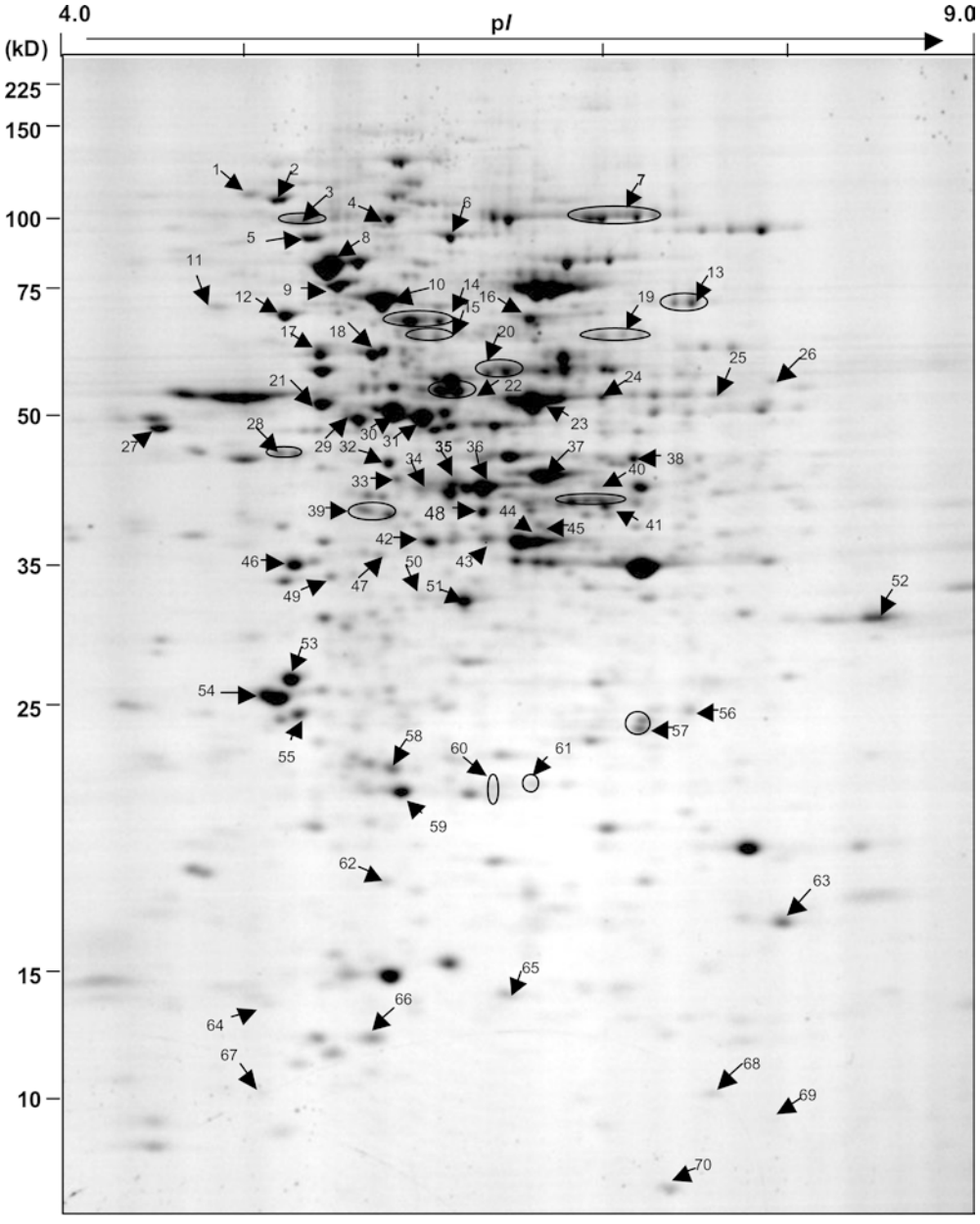

Fig. 3 A representative 2-DE map of 4-day-old *H. pluvialis* cells under favorable growth conditions (the cells were in fresh basal growth medium at 20°C and light of 20 μmol photons m^{-2} s^{-1}). *Arrows* indicate proteins whose abundance varied under oxidative stress (150 μmol photons m^{-2} s^{-1}, 45 mM sodium acetate and 450 μM Fe^{2+}). Numbers correlate with protein identifications listed in Table 2. 2-DE was performed using 250 μg of proteins, linear 18-cm IPG strips (pH 3–10), and a 12% (w/v) total acrylamide SDS secondary dimension. The gel was stained with Coomassie Blue, and image recorded and compared with Z_3 analysis software

Proteins whose abundance underwent changes of at least 2-fold higher or lower than the basal levels in green vegetative cells were regarded to be up-regulated or down-regulated under stress and during the transformation. Group-1 proteins were those that occurred at all stages of the cell cycle and their abundance remained more or less constant throughout 6 days of cultivation under stress. This group represents the richest source of soluble proteins in the cytosol. For example, of 736 proteins resolved from 6 days of stress, 599 were confirmed to be group-1 proteins. Group-2 proteins refer to those whose abundance decreased gradually during the 6 days of stress. Conversely, group-3 includes proteins whose abundance increased throughout the same period of time. Group-4 comprises proteins of abundance being transiently down-regulated, followed by up-regulation during oxidative stress. Group-5 includes proteins whose abundance was transiently up-regulated, followed by down-regulation during oxidative stress.

Identification of proteins with altered expression in response to oxidative stress

Major proteins whose abundance varied considerably during oxidative stress were excised from 2-D gels and subjected to in-gel digestion and MALDI–TOF MS analysis. Positive identification of proteins was made through sequence database searching using the MS-Fit and ProFound algorithms. The NCBI database was entered and the taxonomic category was initially set to green plants. If no significant sequence similarity was found within this narrow species group, all species across taxonomic boundaries were selected. Only can-

Table 1 Protein expression patterns occurring in *Haematococcus pluvialis* during oxidative stress, as resolved by 2-DE

No.	Protein expression pattern[a]	No. of protein spots excised	No. of proteins identified
1	Constantly expressed at all times	599	–
2	Expression was down-regulated during oxidative stress	56	13
3	Expression was up-regulated during oxidative stress	78	19
4	Transient down-regulation followed by up-regulation during oxidative stress	65	8
5	Transient up-regulation followed by down-regulation during oxidative stress	89	31

[a]Proteins regarded to undergo up- or down-regulation during the transformation were those whose abundance varied at least 2-fold higher or lower than the basal levels occurring in green vegetative cells

didates that appeared at the top of the list of both algorithms were considered positive identifications.

Table 2 lists identified proteins with apparently altered abundance during oxidative stress. Overall, 70 protein orthologues were identified, of which 46 were from green plants including 15 from *Chlamydomonas reinhardtii*, a species phylogenetically closely related to *H. pluvialis*. Among the 70 protein orthologues, 13 were down-regulated whereas 19 were up-regulated throughout the 6 days of stress. Moreover, 8 proteins were transiently down-regulated, followed by up-regulation, whereas 30 proteins were transiently up-regulated, followed by down-regulation during the same period of time (Tables 1, 2). These proteins were thought to be involved in a broad range of functions including cellular processes and stress response, central and intermediary metabolism, energy metabolism, biosynthesis of fatty acids, carbohydrate, carotenoids, and amino acids, as well as protein translation, transport and binding. Protein spots whose abundance changed considerably under stress but whose sequences failed to be identified by MALDI–TOF MS analysis were not studied further.

Immediate transient up-regulation of protein expression under stress

Upon stress induction, transient enhancement of protein expression occurred in a large number of protein species. Spots 8 and 9 were identified as heat-shock proteins HSP81-1 and HSP81-3 from *Arabidopsis*, which belong to the HSP90 family (Fig. 3, Table 2). Spot 10 was identified as a DnaK-type molecular chaperone HSP70b precursor from *C. reinhardtii* (Fig. 3, Table 2). Expression of these three molecular chaperone proteins was up-regulated immediately after onset of stress (30 min); ca. a 5-fold increase in Hsp81-3 and a 2-fold increase in Hsp81-1 and DnaK occurred 24 h after the onset of stress, and their expression remained at high levels until 48 h. These proteins returned to their basal levels after 72 h of stress (Fig. 4a). Expression of an isopentenyl-diphosphate δ-isomerase (IPI) orthologue, which participates in biosynthesis of carotenoids and many other long-chain isoprenoids (Cunningham and Gantt 1998), was up-regulated immediately with a 5-fold increase of IPI at 24 h of stress (Fig. 4b). Spot 26 (Figs. 3, 4c) was an orthologue of catalase from *C. reinhardtii*. The basal level of catalase was low in green vegetative cells, but the expression of the enzyme was progressively up-regulated to a maximum level (ca. 6-fold) at 24 h and then gradually down-regulated to the control level after 72 h of stress. Expression of two *Arabidopsis* peroxidase orthologues, peroxidase 10 precursor (P10) and peroxidase 47 precursor (P47) orthologues, was up-regulated immediately after 30 min of oxidative stress. The basal levels of these two peroxidases were fairly high. Oxidative stress only slightly enhanced their expression levels. However, the enhanced regulation was rather short-lived. Down-regulation of the proteins occurred after 4 h of stress, and decreased to below control levels after 16 h of stress (Fig. 5a).

Oxidative stress also resulted in up-regulation of a set of proteins involved in carbohydrate metabolism. A glucose-6-phosphate isomerase (GPI), transaldolase A, and a cytoplasmic form of phosphoglycerate kinase (PGK) were transiently up-regulated and then reverted to down-regulation as stress persisted (Fig. 5a).

Two subunits of tubulin transiently doubled in quantity during the first 12 h of stress, and their amounts dropped afterwards (Fig. 5b). It appeared that accumulation of tubulin subunits might be required for assembling new flagella required for the vigorous reproduction of red motile cells in the early stage of stress induction.

Time-delayed transient up-regulation of antioxidant defense proteins under stress

A chloroplast ascorbate peroxidase orthologue (spot 43 in Fig. 3; Fig. 4b) was identified that showed a delayed up-expression pattern; a transient enhanced expression (ca. 8-fold) did not occur until 24 h and reached maximum level after 48 h of stress.

Spatially differential protein expression among different cellular compartments

The expression of chloroplast ATPase β-subunit was down-regulated slightly during the 6 days of stress, while a mitochondrial ATPase β-subunit was transiently

Table 2 Identified protein orthologues from the green alga *H. pluvialis*, the expression levels of which altered under oxidative stress. *NMP* Number of peptides matched, *SC* sequence coverage

No.	Protein	Accession No.	MW (kDa)	pI	NMP	SC (%)	Mowse score
Down-regulated proteins (13)							
2	Ubiquitin-activating enzyme E1 2	P31251	116.8	5.1	7	14	3.66e+04
3	Aconitate hydratase, cytoplasmic	Q42560	98.2	6.0	7	11	9.39e+04
4	Cell division cycle protein 48	Q96372	89.3	5.1	9	15	6.86e+04
13	Nitrite reductase [NAD(P)H]	P42435	88.4	5.1	10	15	6.22e+04
15	Ferredoxin-nitrite reductase	9968473	64.8	6.3	6	10	8.78e+04
17	Aspartyl-tRNA synthetase	Q8XJ28	68.0	5.1	8	21	3.68e+04
22	Pyruvate kinase	Q9PK61	53.2	5.9	9	23	5.21e+04
28	Flavin-containing monooxygenase	15221214	53.8	5.7	6	15	3.93e+04
32	Eukaryotic initiation factor 4A-9	Q40471	46.8	5.5	9	23	2.39e+06
36	Glutamine synthetase, cytosolic	Q42688	42.1	6.0	6	12	9.51e+03
42	Ketol-acid reductoisomerase 1	Q9UWX9	36.8	6.6	6	18	8.18e+03
48	Phosphoglycerate kinase, chloroplast	1172455	49.0	8.8	5	15	3.21e+03
59	Superoxide dismutase [Mn/Fe]	O54233	15.8	4.9	4	37	2.92e+03
Up-regulated proteins (19)							
7	Phosphoenolpyruvate carboxylase 1	P10490	110.7	6.0	11	17	1.95e+05
20	Glucose-6-phosphate 1-dehydrogenase	Q9FJI5	59.1	6.0	7	22	8.66e+04
33	Actin	P53498	41.8	5.3	11	27	5.16e+04
35	Phosphoglycerate kinase	P46273	45.2	6.1	6	21	3.62e+04
38	Purple acid phosphatase-like protein	15231682	48.5	6.0	6	28	8.51e+03
50	Malate dehydrogenase	7431166	36.6	8.5	4	13	2.16e+03
51	RAS-related protein racE	Q23862	24.4	6.3	5	22	2.02e+04
52	Oxygen-evolving enhancer protein 2	P12853	30.5	8.3	5	18	2.05e+03
53	14-3-3-like protein	P52908	29.5	4.9	6	28	2.84e+04
55	Triosephosphate isomerase	Q59182	27.8	5.9	5	27	1.01e+04
56	Heat-shock 22 kDa protein-like	15242086	23.4	9.0	5	24	1.58e+03
57	Alcohol dehydrogenase 2	P25721	27.7	8.4	5	32	7.96e+03
60	Glutathione *S*-transferase	7381081	20.4	6.0	4	19	2.65e+03
64	Calmodulin-1	115480	16.9	4.1	4	35	3.26e+03
65	Nucleoside diphosphate kinase I	P39207	16.5	6.3	4	41	2.39e+03
66	Ferredoxin $NADP^+$ reductase	294095	10.7	5.0	4	46	4.51e+03
67	Thioredoxin I	P22803	11.2	4.8	4	33	1.02e+03
69	Putative lipid transfer protein	15226046	13.0	9.7	4	38	6.14e+03
70	Ubiquitin	P14624	8.5	6.6	6	44	7.85e+03
Proteins transiently down-regulated, then up-regulated (8)							
5	Oligopeptidase A	P44573	78.0	5.4	6	13	4.26e+04
6	Lipoxygenase	10764845	97.5	5.4	8	11	4.38e+04
16	Glu-ADT subunit E	Q9HJJ6	67.7	5.7	7	20	7.18e+04
18	Protein kinase homolog	7488240	48.2	5.8	5	16	3.07e+03
23	Rubisco large subunit	P00877	52.5	6.1	15	23	3.09e+05
24	Putative alcohol oxidase	16905151	62.9	8.2	7	17	7.28e+04
30	ATP synthase β-subunit	23503629	40.9	5.5	13	32	3.38e+04
31	ATP synthase α-subunit	P30392	55.2	8.9	9	14	2.45e+04
Proteins transiently up-regulated, then down-regulated (30)							
1	Phytochrome	P33529	123.9	5.7	9	10	6.04e+04
8	Heat-shock protein 81-1	P27323	80.6	5.0	11	18	7.80e+04
9	Heat-shock protein 81-3	P51818	80.1	4.9	7	14	2.21e+04
10	dnaK	7441862	72.0	5.3	6	10	7.32e+03
11	H^+-transporting ATP synthase	18415909	59.7	6.2	7	16	2.26e+04
12	ATPase β-chain, mitochondrial	P38482	61.8	5.0	7	13	4.35e+03
14	Vacuolar ATPase subunit A	P31400	68.1	5.1	9	17	5.15e+03
19	6-Phosphogluconate dehydrogenase	15238151	53.3	5.6	9	20	6.38e+05
21	Tubulin β-1/ β-2 chain	P04690	49.6	4.8	17	37	8.89e+06
25	Putative protein disulfide isomerase precursor	15219086	55.6	4.8	7	15	6.42e+04
26	Catalase	7433014	55.9	6.7	8	16	7.38e+04
27	Enolase	Q8TQ79	46.8	4.5	6	18	1.18e+03
29	Tublin α-1 chain	P09204	49.6	5.0	13	36	7.22e+08
34	Glucose-6-phosphate isomerase	1730169	62.7	6.3	8	18	8.42e+03
37	Peroxidase 47 precursor	Q9SZB9	34.6	6.9	5	20	1.10e+04
39	Peroxidase 10 precursor	Q9FX85	38.0	6.2	9	23	6.92e+04
40	L-Lactate dehydrogenase	P47698	34.0	8.8	6	28	3.28e+03
41	Transaldolase A	P78258	35.7	5.9	7	26	8.29e+03
43	Chloroplast ascorbate peroxidase	5804780	33.8	8.5	5	18	7.63e+03
44	Glyceraldehyde 3-phosphate dehydrogenase	P53430	36.4	8.3	5	23	3.88e+03
45	Fructose-bisphosphate aldolase class I	P71295	38.1	6.2	5	19	3.81e+03
46	Probable peroxiredoxin	O58966	24.7	5.6	7	37	3.32e+04

Table 2 (Contd.)

No.	Protein	Accession No.	MW (kDa)	pI	NMP	SC (%)	Mowse score
47	Isopentenyl-diphosphate δ-isomerase	Q99RS7	38.9	5.3	6	12	1.98e+03
49	Phosphatase PP1	5053113	34.8	5.1	5	16	4.72e+03
54	Dephospho-CoA kinase	O34932	22.0	5.1	5	21	5.23e+03
58	Alkyl hydroperoxide reductase	P26427	20.8	5.0	4	33	1.85e+03
61	Superoxide dismutase [Cu–Zn]	Q01137	15.7	6.1	4	40	1.62e+03
62	NADH-plastoquinone oxidoreductase	P06252	19.6	5.9	4	25	1.40e+03
63	Rubisco small subunit 1	P00865	20.1	8.9	4	21	5.95e+03
67	GTP cyclohydrolase I 1	Q9HYG8	20.8	7.0	5	19	3.81e+03

up-regulated and reached its maximum level (ca. 5-fold) after 48 h of stress (Figs. 5b, 4a). In Fig. 3, spot 59 and spot 61 were identified as a mitochondrion-associated manganese-superoxide dismutase (MnSOD) and a cytosol-localized copper/zinc-superoxide dismutase (Cu/ZnSOD), respectively. The expression of MnSOD was constitutively high in vegetative cells and progressively down-regulated after onset of stress, and the protein content was reduced to one-tenth relative to its basal level after 72 h of stress (Fig. 6a). A decrease in MnSOD mRNA levels was also reported in spring wheat when a fully hardened plant was exposed to three nonlethal freeze-thaw sequences (Wu et al. 1999). In contrast, Cu/ZnSOD was present in small quantities in green vegetative cells. Its expression, however, was up-regulated and reached the highest level (ca. 8-fold) at 48 h, and then reduced to only a trace amount after 72 h of stress (Fig. 6a).

Down-regulation of protein expression under stress

Spot 36 in Fig. 4 was identified as a cytoplasmic form of glutamine synthetase (GS1) from *C. reinhardtii*, which was assumed to participate in nitrogen assimilation. This enzyme was reduced by ca. 3-fold during 6 days of stress (Fig. 5a).

A chloroplast form of phosphoglycerate kinase (Fig. 5a) and one cytoplasmic form of aconitase (Fig. 6b) were down-regulated after the onset of stress. In addition, many photosynthesis-associated proteins were down-regulated under stress. For instance, the oxidative stress suppressed the amount of ribulose-1,5-bisphosphate carboxylase/oxygenase (Rubisco) large subunit (RbcL) immediately following stress induction and the protein was at a minimum level (ca. one-eighth of the basal amount) after 12 h of stress. Although the protein expression slowly recovered, its content remained lower than that of the control after 72 h of stress (Fig. 5b).

Discussion

Although the accumulation of secondary carotenoids (as molecular antioxidants) and formation of cysts under oxidative stress is a fairly common survival strategy not only for the model algal system *Haematococcus pluvialis*,

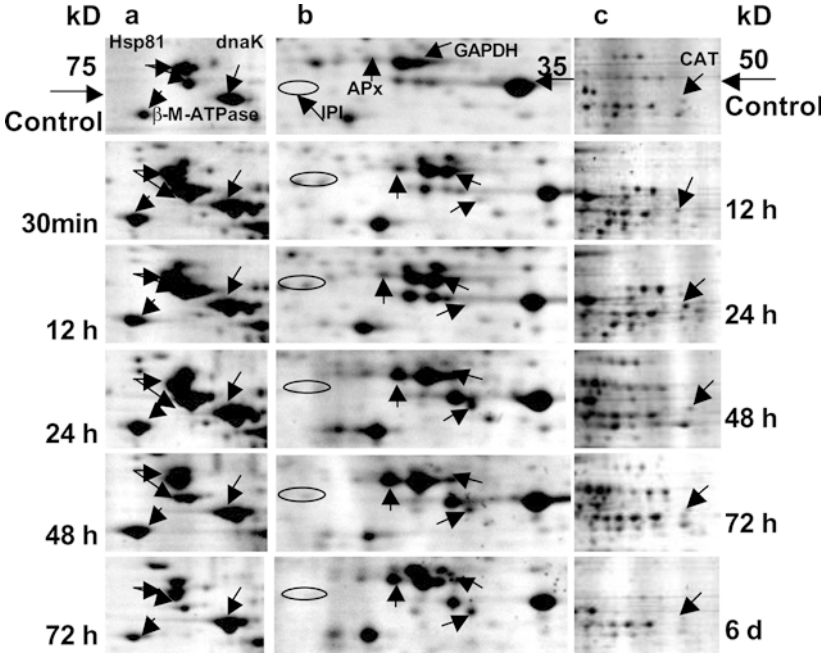

Fig. 4a–c Close-ups of 2-D gels showing the expression of specific proteins as affected by oxidative stress. **a** Transient up-regulation of Hsp 81 isomers (HSP81-1 and HSP81-3), chaperone protein dnaK (DnaK), and mitochondrial ATP synthase β-subunit, (β-M-ATPase). **b** Transient up-regulation of IPI, ascorbate peroxidase (APx), and glyceraldehyde 3-phosphate dehydrogenase (GAPDH). **c** Transient up-regulation of catalase (CAT). The time scale for **b** is the same as that for **a**

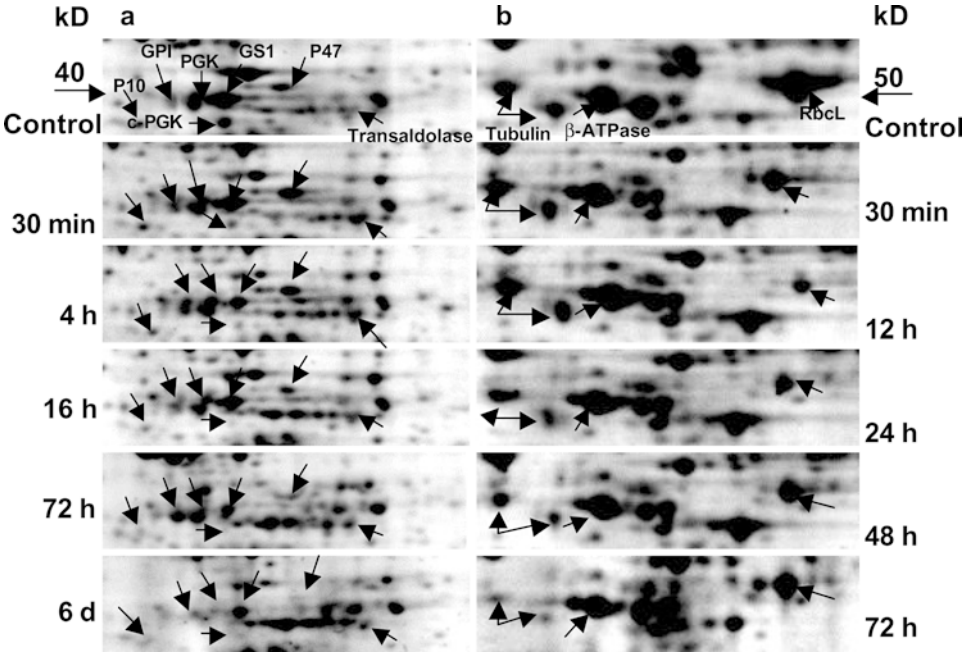

Fig. 5a, b Differential expression of proteins under oxidative stress. **a** Transient up-regulation of cytoplasmic glucose-6-phosphate isomerase (GPI), phosphoglycerate kinase (PGK), transaldolase A, peroxidase 10 precursor (P10), and peroxidase 47 precursor (P47), and at the same time down-regulation of glutamine synthetase (GS1), and phosphoglycerate kinase, chloroplast precursor (c-PGK). **b** Transient up-regulation of α- and β-subunits of tubulin, and transient down-regulation of Rubisco large subunit (RbcL) and chloroplast-associated ATP synthase β-subunit (β-ATPase)

but also for many green algae and other microbes, little is actually known about early molecular defense/adaptation mechanisms occurring upon onset of stress, and before cyst formation and pigment accumulation become evident. In this study, the stress stimuli were excessive amounts of acetate and Fe^{2+}, and high light intensity. It is well established that this combination can induce oxidative stress of *H. pluvialis* through overproduction of ROS, which ultimately induce the formation of astaxanthin-rich cysts as stress persists (Kobayashi et al. 1991, 1993; Steinbrenner and Linden 2001). Although it has been widely assumed that *H. pluvialis* cells may evolve enzymatic and non-enzymatic antioxidant defense systems to cope with oxidative stress, such molecular defense mechanisms are still poorly understood (Boussiba 2000). Our proteomic analysis of global expression patterns of cellular soluble proteins reveals that multiple, concerted enzymatic antioxidative reactions, along with a complex battery of proteins involved in photosynthesis, respiration, nitrogen assimilation, and carotenoid biosynthesis underwent dynamic changes in response to oxidative stress.

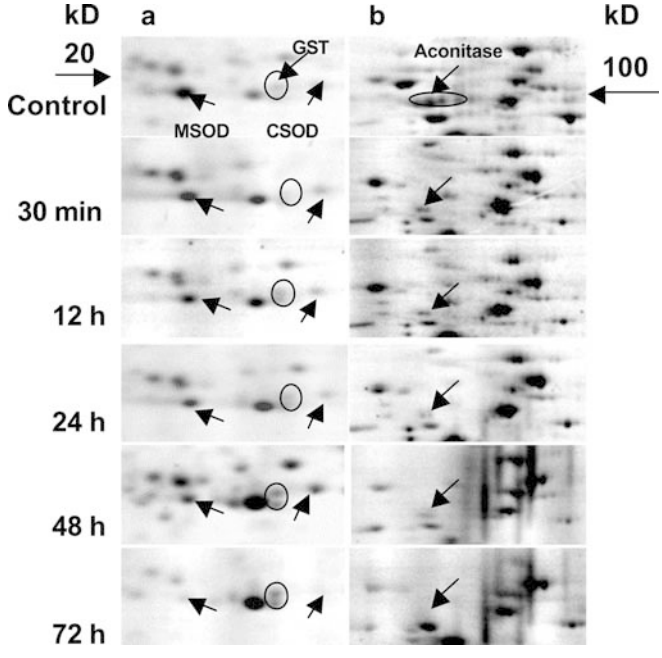

Fig. 6a, b Differential expression of proteins under oxidative stress. **a** Transient up-regulation of glutathione *S*-transferase (GST), and differential expression of mitochondrial superoxide dismutase (MSOD) and cytoplasmic superoxide dismutase (CSOD). **b** Transient down-regulation of aconitase

Up-regulation of SOD and HSP

As the first line of defense against ROS (McCord and Fridovich 1969), the Cu/ZnSOD in *H. pluvialis* underwent transient up-regulation, followed by reverting to its original level during 6 days of stress. In a previous study, Kobayashi et al. (1997) reported that Cu/ZnSOD activity was detected in vegetative cells but showed little activity in the mature cyst cells of *H. pluvialis*. The conflicting results from the two studies may be due to the different physiological status of the cells under study. Our analysis was made with the cells harvested at different time intervals for up to 72 h, but the cells used by Kobayashi's group for measurement of Cu/ZnSOD activities were from 4-day-old (96 h) cultures, in which the Cu/ZnSOD might already have been in the down-regulation phase. An increase in Cu/ZnSOD activity, in conjunction with a simultaneous decrease in MnSOD activity, was also found in cowpea under salt stress (Hernandez et al. 1998). The transient enhanced

expression of Cu/ZnSOD implies that the cytosol may be an active radical-quenching site in *H. pluvialis* under stress. In addition to eliminating excess superoxide, Cu/ZnSOD was reported to raise cytoplasmic levels of H_2O_2 during oxidative stress, which may in turn activate cellular defense mechanisms (Tsang et al. 1991).

In addition to the HSP81-1, HSP81-3 and DnaK orthologues identified in this study, we detected two other heat-shock proteins, HSP70 and HSP60, from the cell wall of *H. pluvialis* (Wang et al. 2004). In contrast to other major heat-shock proteins, HSP81-1 and HSP81-3 are also expressed in green vegetative cells. This phenomenon was also observed in *Arabidopsis* at normal growth temperature (Yabe et al. 1994). Exogenous application of 10 mM indole-3-acetic acid (IAA) and 0.1 M NaCl to *Arabidopsis* significantly enhanced the accumulation of HSP81-3 mRNA transcripts while the HSP81-1 transcript accumulation only slightly increased (Yabe et al. 1994). High basal levels of these proteins under normal growth conditions suggest that their expression is necessary at all times to provide adequate protection. HSPs are thought to have a rather nonspecific but nevertheless important protective function under stress to ensure cell viability regardless of the specific stress stimulus (Bernhardt et al. 2003).

Up-regulation of mitochondrial respiratory proteins under oxidative stress

In contrast to the suppression of chloroplast β-ATPase subunit under stress, the mitochondrial β-ATPase subunit was transiently up-regulated and the highest amount of the protein occurred at 48 h following stress induction. This finding is in agreement with earlier physiological evidence that the respiration rate transiently increases during the transformation of green vegetative cells to red cysts in this organism (Tan et al. 1995). Increased mitochondrial respiratory activities during the transition may facilitate the energy-dependent build up of the antioxidative defense pathways, as well as accelerating degradation of macromolecules such as chlorophylls, proteins and lipids associated with 'excessive' thylakoid membranes that can otherwise impose negative effects on the cells.

Up-regulation of carotenoid biosynthetic enzymes under oxidative stress

Isopentenyl-diphosphate δ-isomerase (IPI) is a soluble enzyme that occurs in plastids and cytosol of microalgae and plants that catalyzes the reversible isomerization of isopentenyl pyrophosphate (IPP) to produce dimethylallyl pyrophosphate (DMAPP; Cunningham and Gantt 1998). An increase in the activity of IPI was correlated with the increased biosynthesis of carotenoids in developing plastids of maize, and was regarded as a crucial rate-limiting step leading to the biosynthesis of carotenoids (Cunningham and Gantt 1998). About a 3-fold increase in the carotenoid/chlorophyll ratio was reported as a result of the expression of one of two IPIs, which was differentially up-regulated in *H. pluvialis* by higher light intensity (Sun et al. 1998). In our study, the maximum expression of IPI occurred at 24 h and then down-regulated as stress persisted, although the astaxanthin accumulation continued throughout the 6 days of cultivation. This suggests that IPI may have a low turnover rate, thereby ensuring long-lasting activity in facilitating astaxanthin biosynthesis. Interestingly, a similar correlation between the expression of another carotenoid biosynthesis enzyme, phytoene desaturase, and the biosynthesis of astaxanthin was found in this organism under stress conditions (Grunewald et al. 2000). However, most of the enzymes that catalyze astaxanthin biosynthesis were not detected because they are membrane-bound. Difficulties of isolation and separation of membrane-bound proteins using our current 2-DE method prevented us from investigating membrane proteins at this stage.

Up-regulation of carbohydrate metabolism proteins under oxidative stress

Most of the proteins involved in glycolysis, including glucose-6-phosphate isomerase, aldolase, triose phosphate isomerase, glyceraldehyde 3-phosphate dehydrogenase, phosphoglycerate kinase, enolase, lactate dehydrogenase and alcohol dehydrogenase were up-regulated or transiently up-regulated during 6 days of oxidative stress. While pyruvate kinase, which catalyzes the formation of pyruvate from phosphoenolpyruvate with the concomitant synthesis of ATP from ADP, was down-regulated in *H. pluvialis* under oxidative stress, the other two enzymes, phosphoenolpyruvate carboxylase and malate dehydrogenase, which together with the malic enzyme can bypass the reaction catalyzed by pyruvate kinase (Dennis et al. 1997), were up-regulated. In addition, three enzymes of the pentose phosphate pathway, i.e., glucose-6-phosphate 1-dehydrogenase (GPDH), 6-phosphogluconate dehydrogenase (PGDH) and transaldolase (TA), were up-regulated in *H. pluvialis* in response to stress. It has been suggested that during stress the pentose phosphate pathway may serve as a key source for reduced NADPH for ROS removal (Pandolfi et al. 1995). In addition, higher levels of NADPH may be required for the biosynthesis of lipids (Koehler and Van Noorden 2003), which are the major constituents of the lipid bodies that accumulate in red cysts.

The cytoplasmic aconitase was down-regulated in *H. pluvialis* under stress. It was shown that this enzyme was inhibited in tobacco by NO (Navarre et al. 2000) and inhibited in potato by H_2O_2 (Verniquet et al. 1991). Aconitase is an iron–sulfur (4Fe–4S)-containing enzyme that catalyzes the reversible isomerization of citrate to

isocitrate (Peyret et al. 1995). The enzyme has two isoforms, one is located in mitochondria and the other in the cytosol. In plants, cytoplasmic aconitase and mitochondrial aconitase show similar characteristics and cannot be differentiated (Brouquisse et al. 1987). The decrease in mitochondrial aconitase level is likely to impose significant flux restrictions on the tricarboxylic acid (TCA) cycle and the electron transport chain, which in turn may increase citrate concentration. It was reported that higher levels of citrate enhance the alternative oxidase pathway, thereby reducing ROS production (Navarre et al. 2000).

The principle function of the glycolytic pathway in plants is to provide intermediates for biosynthetic pathways (Dennis et al. 1997). The up-regulation of proteins involved in glycolysis and down-regulation of proteins in the TCA cycle indicate redirection of a substantial amount of the cell's carbon resource into other biosynthetic pathways such as cell wall biosynthesis and lipid body formation in *H. pluvialis*.

Down-regulation of photosynthetic proteins under stress

Suppression of photosynthetic activity is thought to be one of the consequences of cellular response to stress conditions (Zlotnik et al. 1993; Lu et al. 1994; Tan et al. 1995). Our 2-D gels clearly indicate that the expression of RbcL, phosphoglycerate kinase and ATPase was down-regulated under stress. It was reported that transfer of *C. reinhardtii* cells from low light to high light intensities resulted in a noticeable transient suppression of the expression of RbcL (Shapira et al. 1997). Accordingly, the synthesis of the protein was reduced after 15 min and almost completely lost after 2 h of high light stress. Partial restoration of RbcL synthesis did not occur until 6 h following the stress. In barley, oxidative treatment was shown to stimulate the association of Rubisco with the insoluble fraction of chloroplasts and partial proteolysis of RbcL, suggesting that the increase in amount of ROS generated by O_2 reduction at photosystem I might trigger Rubisco degradation (Desimone et al. 1996). Interestingly, Rubisco small subunit (RbcS) was somewhat up-regulated after the onset of stress. Similar results were found in *C. reinhardtii* in which the RbcL was reduced by high light within 2 h, whereas the RbcS was not affected within 15 min and was up-regulated at 2 h (Shapira et al. 1997). It should be noted that RbcL is encoded by the chloroplast genome whereas RbcS is encoded by the nuclear genome.

Since many of the photosynthetic components are functionally linked, reduction of any of these components may lead to the overall suppression of photosynthetic activity (Haake et al. 1998). Because the chloroplast is one of the major sources of ROS production in photosynthetic cells, the physiological significance of suppression of photosynthetic activity under stress conditions would likely be to reduce the production of ROS.

Down-regulation of nitrogen assimilation proteins under oxidative stress

The cytoplasmic glutamine synthetase (GS1) from *C. reinhardtii* catalyzes the ATP-dependent assimilation of ammonium to glutamine, using glutamic acid as its substrate (Chen and Silflow 1996). This protein orthologue identified in *H. pluvialis* was down-regulated during 6 days of stress. Aflalo et al. (1999) reported that inhibition of GS1 activity by the herbicide BASTA led to the accumulation of astaxanthin in *H. pluvialis*. It has been documented that nitric oxide (NO), an intermediate of nitrogen assimilation, is a reactive radical that acts, like ROS, as an oxidative agent. Furthermore, nitrite oxide may react with superoxide anion in the cytosol to form an even more oxidatively active molecule, peroxynitrite. Therefore, the down-regulation of GS1 should be another protective mechanism for *H. pluvialis* survival under oxidative stress.

Antioxidant enzymes versus antioxidant astaxanthin

Our results reveal that a majority of the antioxidative enzymes identified in this organism underwent transient up-regulation under oxidative stress, and their responses were either immediate or time-delayed. However, sooner or later within the first 2 days of stress, most of these enzymes reverted to either their basal levels or below. The roles of these enzymes in antioxidative defense pathways are reduced as the stress persists. Since dynamic changes in antioxidative enzymes occurred within the first 12–48 h of the application of stress, and prior to the cellular accumulation of astaxanthin and the visible morphological and cellular structural changes, we believe that our results represent, in effect, the early events of the stress response (a primary defense response to oxidative stress), as well as those that occur during the transition to cyst formation that comes with continuing stress.

The cellular antioxidant astaxanthin begins to be synthesized about 12 h after stress induction, accumulates in a linear mode for 3–4 days and reaches a maximum level (ca. 2.0% cell dry weight) on day 6. Given that an antioxidant role of astaxanthin has been confirmed in *H. pluvialis* (Kobayashi et al. 1997; Kobayashi 2000) and in the yeast *Phaffia* (Schroeder and Johnson 1995), it is suggested that the antioxidant astaxanthin molecules may largely replace the antioxidative enzymes to protect mature cysts of *H. pluvialis* under oxidative stress conditions. Thus, *Haematococcus* cells may have evolved different cellular/molecular defense mechanisms (e.g., primary- and secondary-defense strategies) to cope with either short-term or long-term stress conditions. Our proteomic analysis of global expression of *H. pluvialis* soluble proteins supports the hypothesis of Kobayashi et al. (1997) that the organism has two antioxidative mechanisms, antioxidative enzymes in vegetative cells and antioxidative astaxanthin in cyst cells. Furthermore, it has revealed highly complex, dynamic

enzymatic defense reactions occurring upon onset of stress, and before cyst formation and pigment accumulation is evident. It is the multiple antioxidative enzymes and antioxidant astaxanthin acting in concert, both spatially and temporally, that facilitate cell transformation under oxidative stress.

Acknowledgements We thank Dr. Ken Hoober for his encouragement and advice, and Dr. Dan Brune for assistance with MALDI–TOF mass spectrometry analysis. The US National Science Foundation (Grant CHE-0131222) is gratefully acknowledged for providing funding for the mass spectrometer used in this work.

References

Aflalo C, Bing W, Zarka A, Boussiba S (1999) The effect of the herbicide glufosinate (BASTA) on astaxanthin accumulation in the green alga *Haematococcus pluvialis*. Z Naturforsch 54c:49–54

Asada K (1994) Production and action of active oxygen species in photosynthetic tissues. In: Foyer CH, Mullineaux PM (eds) Causes of photooxidative stress and amelioration of defense systems in plants. CRC, Boca Raton, FL, pp 77–104

Bernhardt J, Weibezahn J, Scharf C, Hecker M (2003) *Bacillus subtilis* during feast and famine: visualization of the overall regulation of protein synthesis during glucose starvation by proteome analysis. Genome Res 13:224–237

Blokhina O, Virolainen E, Fagerstedt KV (2003) Antioxidants, oxidative damage and oxygen deprivation stress: a review. Ann Bot 91:179–194

Boussiba S (2000) Carotenogenesis in the green alga *Haematococcus pluvialis*: cellular physiology and stress response. Physiol Plant 108:111–117

Boussiba S, Bing W, Yuan JP, Zarka A, Chen F (1999) Changes in pigments profile in the green alga *Haematococcus pluvialis* exposed to environment stresses. Biotech Lett 21:601–604

Breitenbach J, Fernandez-Gonzalez B, Vioque A, Sandmann G (1998) A higher-plant type ζ-carotene desaturase in the cyanobacterium *Synechocystis* PCC6803. Plant Mol Biol 36:725–732

Brouquisse R, Nishimura M, Gaillard J, Douce R (1987) Characterization of a cytoplasmic aconitase in higher-plant cells. Plant Physiol 84:1402–1407

Chen Q, Silflow CD (1996) Isolation and characterization of glutamine synthetase genes in *Chlamydomonas reinhardtii*. Plant Physiol 112:987–996

Cunningham FX, Gantt E (1998) Genes and enzymes of carotenoid biosynthesis in plants. Annu Rev Plant Physiol Plant Mol Biol 49:557–583

Dennis DT, Huang Y, Negm FB (1997) Glycolysis, the pentose phosphate pathway and anaerobic respiration. In: Dennis DT, Turpin DH, Lefebvre DD, Layzell DB (eds) Plant metabolism. Longman, Harlow, pp 105–123

Desikin R, Mackerness SAH, Hancock JT, Neill SJ (2001) Regulation of the *Arabidopsis* transcriptome by oxidative stress. Plant Physiol 127:159–172

Desimone M, Henke A, Wagner E (1996) Oxidative stress induces partial degradation of the large subunit of ribulose-1,5-bisphosphate carboxylase/oxygenase in isolated chloroplasts of barley. Plant Physiol 111:789–796

Foyer CH, Mullineaux PM (eds) (1994) Causes of photooxidative stress and amelioration of defense systems in plants. CRC, Boca Raton

Grunewald K, Hagen C, Braune W (1997) Secondary carotenoid accumulation in flagellates of the green alga *Haematococcus lacstris*. Eur J Phycol 32:387–392

Grunewald K, Eckert M, Hirschberg J, Hagen C (2000) Phytoene desaturase is localized exclusively in the chloroplast and up-regulation at the mRNA level during accumulation of secondary carotenoids in *Haematococcus pluvialis* (Volvocales, Chlorophyceae). Plant Physiol 122:1261–1268

Haake V, Zrenner R, Sonnewald U, Stitt M (1998) A moderate decrease of plastid aldolase activity inhibits photosynthesis, alters the levels of sugars and starch and inhibits growth of potato plants. Plant J 14:147–157

Hernandez JA, Almansa MS, DelRío LA, Sevilla F (1998) Effect of salinity on metalloenzymes of oxygen metabolism in two leguminous plants. J Plant Nutr 16:2539–2554

Hershkovits G, Dubinsky Z, Katcoff DJ (1997) A novel homologue of the prokaryotic *htrA* gene is differentially expressed in the alga *Haematococcus pluvialis* following stress. Mol Gen Genet 254:345–350

Kobayashi M (2000) In vivo antioxidant role of astaxanthin under oxidative stress in the green alga *Haematococcus pluvialis*. Appl Microbiol Biotechnol 54:550–555

Kobayashi M, Kakizono T, Nagai S (1991) Astaxanthin production by a green-alga, *Haematococcus-pluvialis* accompanied with morphological-changes in acetate media. J Ferment Bioeng 71:335–339

Kobayashi M, Kakizono T, Nagai S (1993) Enhanced carotenoid biosynthesis by oxidative stress in acetate-induced cyst cells of a green unicellular alga *Haematococcus pluvialis*. Appl Environ Microbiol 59:867–873

Kobayashi M, Kakizono T, Nishio N, Kurimura Y, Tsuji Y (1997) Antioxidant role of astaxanthin in the green alga *Haematococcus pluvialis*. Appl Microbiol Biotechnol 48:351–356

Koehler A, Van Noorden CJ (2003) Reduced nicotinamide adenine dinucleotide phosphate and the higher incidence of pollution-induced liver cancer in female flounder. Environ Toxicol Chem 22:2703–10

Linden H (1999) Carotenoid hydroxylase from *Haematococcus pluvialis*: cDNA sequence, regulation and functional complementation. Biochim Biophys Acta 1446:203–212

Lotan T, Hirschberg J (1995) Cloning and expression in *Escherichia coli* of the gene encoding β-4-C-oxygenase, that converts β-carotene to the ketocarotenoid canthaxanthin in *Haematococcus pluvialis*. FEBS Lett 364:125–128

Lu F, Vonshak A, Boussiba S (1994) Effect of temperature and irradiance on growth of *Haematococcus pluvialis* (Chlorophyceae). J Phycol 30:829–833

McCord JM, Fridovich I (1969) Superoxide dismutase: an enzymatic function for erythrocuprein (hemocuprein). J Biol Chem 244:6049–6055

Mittler R (2002) Oxidative stress, antioxidants and stress tolerance. Trends Plant Sci 7:405–410

Navarre DA, Wendehenne D, Durner J, Noad R, Klessig DF (2000) Nitric oxide modulates the activity of tobacco aconitase. Plant Physiol 122:573–583

Pandolfi PP, Sonati F, Rivi R, Mason P, Grosveld F, Luzzatto L (1995) Target disruption of the housekeeping gene encoding glucose 6-phosphate dehydrogenase (G6PD): G6PD is dispensable for pentose synthesis but essential for defense against oxidative stress. EMBO J 14:5209–5215

Peyret P, Perez P, Alric M (1995) Structure, genomic organization, and expression of the *Arabidopsis thaliana* aconitase gene. J Biol Chem 270:8131–8137

Schroeder W, Johnson EA (1995) Singlet oxygen and peroxyl radicals regulate carotenoid biosynthesis in *Phaffia-rhodozyma*. J Biol Chem 270:18374–18379

Shapira M, Lers A, Heifetz PB, Irihimovitz V, Osmond CB, Gillham NW, Boynton JE (1997) Differential regulation of chloroplast gene expression in *Chlamydomonas reinhardtii* during photoacclimation: light stress transiently suppresses synthesis of the Rubisco LSU protein while enhancing synthesis of the PS II D1 protein. Plant Mol Biol 33:1001–1011

Smilansky Z (2001) Automatic registration for images of two-dimensional protein gels. Electrophoresis 22:1616–1626

Steinbrenner J, Linden H (2001) Regulation of two carotenoid biosynthesis genes coding for phytoene synthase and carotenoid hydroxylase during stress-induced astaxanthin formation in the green alga *Haematococcus pluvialis*. Plant Physiol 125:810–817

Steinbrenner J, Linden H (2003) Light induction of carotenoid biosynthesis genes in the green alga *Haematococcus pluvialis*: regulation by photosynthetic redox control. Plant Mol Biol 52:343–356

Sun ZR, Cunningham FX, Gantt E (1998) Differential expression of two isopentenyl pyrophosphate isomerases and enhanced carotenoid accumulation in a unicellular chlorophyte. Proc Natl Acad Sci USA 95:11482–11488

Tan S, Cunningham FX, Youmans M, Grabowski B, Sun Z, Gantt E (1995) Cytochrome *f* loss in astaxanthin-accumulating red cells of *Haematococcus pluvialis* (Chlorophyceae): comparison of photosynthetic activity, photosynthetic enzymes, and thylakoid membrane polypeptides in red and green cells. J Phycol 31:897–905

Tsang EWT, Bowler C, Herouart D, Camp WV, Villarroel R, Genetello C, Montagu MV, Inze D (1991) Differential regulation of regulation of superoxide dismutases in plants exposed to environmental stress. Plant Cell 3:783–792

Verniquet F, Gaillard J, Neuburger M, Douce R (1991) Rapid inactivation of plant aconitase by hydrogen peroxide. Biochem J 176:643–648

Wang SB, Hu Q, Sommerfeld M, Chen F (2003) An optimized protocol for isolation of soluble proteins from microalgae for two-dimensional gel electrophoresis analysis. J Appl Phycol 15:485–496

Wang SB, Hu Q, Sommerfeld M, Chen F (2004) Cell wall proteomics of the green alga *Haematococcus pluvialis* (Chlorophyceae). Proteomics 4:692–708

Wu G, Wilen RW, Robertson AJ, Gusta LV (1999) Isolation, chromosomal localization, and differential expression of mitochondrial manganese superoxide dismutase and chloroplastic copper/zinc superoxide dismutase genes in wheat. Plant Physiol 120:513–520

Yabe N, Takahashi T, Komeda Y (1994) Analysis of tissue-specific expression of *Arabidopsis thaliana* HSP90-family gene HSP81. Plant Cell Physiol 35:1207–1219

Yuan JP, Gong XD, Chen F (1997) Separation and analysis of carotenoids and chlorophyll in *Haematococcus lacustris* by high-performance liquid chromatograph photodiode array detection. J Agric Food Chem 45:1952–1956

Zhekisheva M, Boussiba S, Khozin-Goldberg I, Cohen Z (2002) Accumulation of oleic acid in *Haematococcus pluvialis* (Chlorophyceae) under nitrogen starvation or high light is correlated with that of astaxanthin esters. J Phycol 38:325–331

Zlotnik IS, Sukenik A, Dubinsky Z (1993) Physiological and photosynthetic changes during the formation of red aplanospores in the chlorophyte *Haematococcus pluvialis*. J Phycol 29:463–469